


## Extending the Quantum Coherence of a Near-Surface Qubit by Coherently Driving the Paramagnetic Surface Environment

Dolev Bluvstein, Zhiran Zhang, Claire A. McLellan, Nicolas R. Williams, and Ania C. Bleszynski Jayich  
*Department of Physics, University of California, Santa Barbara, California 93106, USA*

 (Received 15 May 2019; published 4 October 2019)

Surfaces enable useful functionalities for quantum systems, e.g., as interfaces to sensing targets, but often result in surface-induced decoherence where unpaired electron spins are common culprits. Here we show that the coherence time of a near-surface qubit is increased by coherent radio-frequency driving of surface electron spins, where we use a diamond nitrogen-vacancy (NV) center as a model qubit. This technique is complementary to other methods of suppressing decoherence and, importantly, requires no additional materials processing or control of the qubit. Further, by combining driving with the increased magnetic susceptibility of the double-quantum basis, we realize an overall fivefold sensitivity enhancement in NV magnetometry. Informed by our results, we discuss a path toward relaxation-limited coherence times for near-surface NV centers. The surface-spin driving technique presented here is broadly applicable to a wide variety of qubit platforms afflicted by surface-induced decoherence.

DOI: [10.1103/PhysRevLett.123.146804](https://doi.org/10.1103/PhysRevLett.123.146804)

Decoherence of quantum systems near surfaces is an outstanding challenge that has not been met. Whereas many quantum systems benefit from a high degree of environmental control and regularity, such as atoms trapped in vacuum far from surfaces and atomic-scale defects buried deep in a bulk crystal, interfaces can add important functionality toward scalability, transduction, and networking. However, interfaces also add an uncontrolled element to the qubit's environment. Surfaces, in particular, are inevitable for superconducting qubits, nanomechanical resonators, adatom qubits, atom and ion chip traps, and high spatial resolution sensing, but frequently host sources of decoherence [1–6]. In particular, fluctuating magnetic fields from surface electron spins are implicated as a major source of decoherence for qubits near surfaces [7–13].

The negatively charged nitrogen-vacancy (NV) center in diamond is a renowned, model example of a solid-state qubit [14]. Near-surface NV centers are used as versatile, high spatial resolution quantum sensors [15–18] and are also useful for storing, processing, and transferring quantum information in hybrid quantum systems [19–21]. The NV coherence time is a key parameter in these quantum applications, as it directly limits the possible storage and processing time, as well as the achievable sensitivity in sensing [22,23]. For these applications, it is vital that the NV center reside in close proximity to the diamond surface, as the NV depth determines the coupling strength to other quantum elements, as well as the signal strength and spatial resolution in imaging [24,25]. However, as for a wide variety of other quantum systems, decoherence associated with the surface is a key obstacle in NV-based technologies [12,26,27].

Several approaches are commonly taken to mitigate decoherence of near-surface qubits. Surface engineering is a direct, materials-based approach, which often involves preparing the surface with a host of material-specific protocols [28–31]. Although surface engineering is a promising approach that directly targets the source of the problem, discovering the correct protocols can require painstaking characterization and trial and error; to date, state-of-the-art techniques have not succeeded in completely eliminating the decoherence sources. Further, the surface can degrade in time after the initial preparation, due to spontaneous chemical or structural changes, as well as accumulated surface adsorbates [32–35]. Quantum control of the near-surface qubit is another approach to mitigating decoherence. Dynamical decoupling is a primary example, where by fast rotation the qubit is made insensitive to slower frequencies of fluctuations [36–38]. One can also use qubit states with “clock transitions” that are insensitive to specific perturbations, such as magnetic fields [39–42]. Although they can increase coherence time, these techniques significantly constrain the qubit and its applications, rendering it insensitive to signals that are similar in nature to the noise being decoupled. An active approach that directly addresses only the offending source and leaves the qubit unconstrained, without painstaking materials processing or susceptibility to surface degradation, is a promising path forward.

In this Letter, we demonstrate that coherent radio-frequency driving of surface electron spins removes their decohering effect on nearby qubits. Here we use a diamond NV center as a model near-surface qubit. Importantly, the qubit coherence time increases without any additional

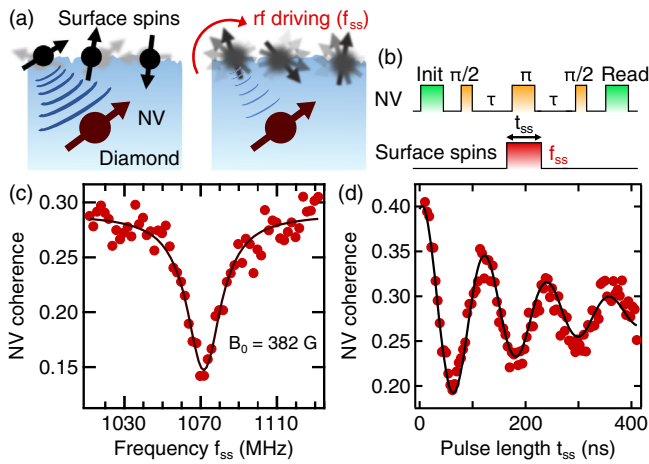


FIG. 1. (a) Schematic of experiment. Near-surface NV centers are dephased by fluctuating magnetic fields (blue contours) from surface electronic spins. Driving the surface spins can suppress NV dephasing. (b) Pulse sequence used in (c) and (d) for probing surface spins. Microwave pulses (yellow and red) are used for spin control, and green illumination pulses are used for initializing and reading the NV spin. When an on-resonance  $\pi$  pulse inverts the surface spins, their quasistatic magnetic field is recoupled and induces NV dephasing. (c) NV coherence as a function of pulse frequency  $f_{SS}$ , showing a resonance corresponding to  $g = 2$  electronic spins. A  $\pi$  pulse of duration  $t_{SS} = 108$  ns is used. Black curve is a Lorentzian fit. (d) NV coherence as a function of pulse length  $t_{SS}$  with  $f_{SS} = 1071$  MHz. Black curve is a fit to exponentially damped Rabi oscillations with  $T_{2,\text{Rabi}} = 200(10)$  ns.  $2\tau$  is  $20 \mu\text{s}$  in (c) and (d) and the NV depth is  $7.5(3)$  nm.

materials processing or manipulation of the qubit. The physical principle of this approach is that, by driving the surface spins sufficiently fast, their interaction with the qubit averages away [Fig. 1(a)], analogous to the phenomenon of motional narrowing [43]. With NV centers specifically, we realize a fivefold enhancement in measurement sensitivity by combining surface-spin driving with the increased magnetic susceptibility of the double-quantum basis. We find the coherence extension from driving is robust among individual NVs. The techniques here are broadly applicable to qubits affected by paramagnetic environments and are directly complementary to other methods of suppressing decoherence. Lastly, we discuss a path toward realizing relaxation-limited coherence times for near-surface NV centers by combining surface-spin driving with existing materials processing techniques.

The experimental setup consists of a home-built, room-temperature confocal microscope for optically addressing individual near-surface NV centers in a single-crystal diamond plate. Three separate radio-frequency (rf) signal generators are used for controlling the electronic spin state of the NV spin qubit, formed by  $|m_s = 0\rangle_{\text{NV}}$  and  $|m_s = \pm 1\rangle_{\text{NV}}$ , as well as the electronic spin state of surface-spin qubits, formed by  $|\uparrow\rangle_{\text{SS}}$  and  $|\downarrow\rangle_{\text{SS}}$ . A single microwave

waveguide patterned on the diamond is used to deliver all rf signals.

The diamond substrate used here is prepared by chemical vapor deposition growth of a 50-nm-thick 99.99%  $^{12}\text{C}$  layer onto an Element Six electronic grade (100) diamond. NV centers are then formed by 4 keV  $^{14}\text{N}$  ion implantation with a dosage of  $5.2 \times 10^{10}$  ions/cm $^2$  into the diamond plate, followed by annealing in vacuum at 850  $^\circ\text{C}$  for 2.5 h. The surface is then triacid cleaned and annealed in an oxygen atmosphere [44] (see Supplemental Material Note 1 for further details [45]). The NV centers' depths are experimentally measured via surface proton NMR and range between  $\sim 4$  and 17 nm [49]. In Supplemental Material Note 2 we estimate a surface-spin density of 0.01–0.1/nm $^2$  [45].

The electron spins at the diamond surface and their interactions with single, shallow NV centers can be probed by a double electron electron resonance (DEER) measurement sequence [Fig. 1(b)], in which the NV center serves as a local, optically addressable readout for a small number of proximal dark spins [50–52]. Specifically, a Hahn echo sequence is performed on the NV, in which a resonant  $\pi$  pulse on the  $|m_s = 0 \rightarrow -1\rangle_{\text{NV}}$  transition decouples the NV center from slowly varying environmental fluctuations that lead to decoherence; simultaneously, a coherent microwave pulse tuned to the surface spins (frequency  $f_{SS}$ ) selectively recouples their quasistatic contribution and leads to NV decoherence. Therefore, in this DEER measurement, the NV coherence serves as a readout for the surface spins.

In Figs. 1(c) and 1(d), we probe the surface-spin frequency- and time-domain response to rf fields using the DEER measurement sequence in Fig. 1(b). Here we use spin-dependent photoluminescence to measure NV coherence in the single-quantum basis  $\{|m_s = 0\rangle, |m_s = -1\rangle\}_{\text{NV}}$  at a fixed echo time  $2\tau$ . The plotted NV coherence is defined as the difference between the populations of the  $|m_s = 0\rangle_{\text{NV}}$  and  $|m_s = -1\rangle_{\text{NV}}$  states after the final  $\pi/2$  pulse in Fig. 1(b) (neglecting the nonunity spin polarization [45]). Figure 1(c) shows the surface-spin electron spin resonance spectrum, obtained by measuring NV coherence as the frequency  $f_{SS}$  of a fixed-duration surface-spin pulse is varied. A clear spin resonance is seen at 1071 MHz, which is the expected resonance for  $g = 2$  spins at the applied magnetic field of  $B_0 = 382$  G; these are the dominant spins for near-surface NVs [52,53] and are the focus of this work. Figure 1(d) shows time-domain Rabi oscillations of the surface spins, obtained by fixing  $f_{SS} = 1071$  MHz and varying the duration  $t_{SS}$  of the surface-spin pulse, demonstrating our ability to address and coherently control these  $g = 2$  surface spins.

Having identified surface spins and established their coherent control, we now show that by coherently driving them we remove their decohering effect on a near-surface qubit. In Fig. 2(c) we observe an increase in the NV Hahn echo  $T_2$  in both the SQ and DQ bases by continuously

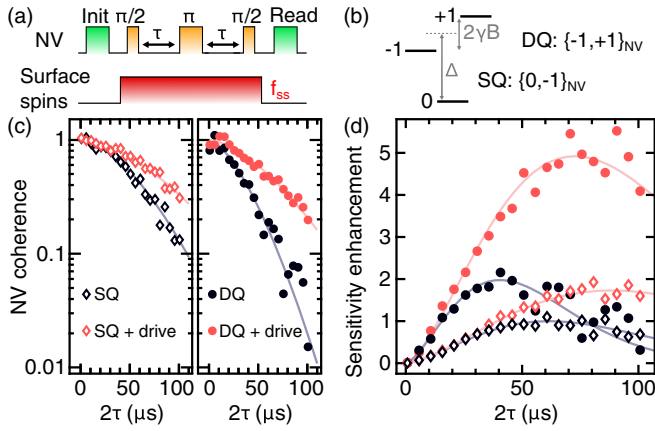


FIG. 2. (a) NV Hahn echo sequence with continuous surface-spin drive, used in (c). (b) NV ground-state spin-1 energy level diagram. The double-quantum (DQ) basis  $\{-1, +1\}_{NV}$  is insensitive to common-mode  $\Delta$  fluctuations and has greater magnetic field  $B$  susceptibility than the single-quantum (SQ) basis  $\{0, -1\}_{NV}$ . (c) NV Hahn echo  $T_2$  coherence decay measured in the SQ (left) and DQ (right) bases, with and without surface-spin driving, showing that driving extends coherence. Data are fit to  $\exp[-(2\tau/T_2)^n]$  with fitted  $n \approx 1.6$ .  $T_{2,SQ} = 65(2) \mu\text{s}$  (dark diamonds),  $T_{2,SQ+drive} = 94(2) \mu\text{s}$  (red diamonds),  $T_{2,DQ} = 41(3) \mu\text{s}$  (dark circles),  $T_{2,DQ+drive} = 75(3) \mu\text{s}$  (red circles). Surface spin  $\Omega_{\text{Rabi}}/2\pi = 10$  MHz and the NV depth is 12.8(3) nm. (d) Enhancement of the NV center's sensitivity to magnetic field variance, calculated for the data in (c) as compared to the peak sensitivity for SQ without drive. A  $5\times$  sensitivity enhancement is observed for the DQ + drive measurement.

driving the surface spins on resonance throughout the echo sequence [sequence in Fig. 2(a)]. Single-tone pulses from two separate rf generators are used to control the NV ground-state spin triplet in either the SQ basis  $\{0, -1\}_{NV}$  or DQ basis  $\{-1, +1\}_{NV}$  (see Supplemental Material Note 3 for further details [45]). As diagrammed in Fig. 1(a), by coherently driving these spins sufficiently fast, their magnetic interaction with the NV averages away and surface-spin-induced dephasing is suppressed. For the NV in Fig. 2, the SQ  $T_2$  increases from 65(2) to 94(2)  $\mu\text{s}$  by driving and the DQ  $T_2$  increases from 41(3) to 75(3)  $\mu\text{s}$  by driving. Here we drive the surface spins at  $\Omega_{\text{Rabi}}/2\pi = 10$  MHz, which is roughly  $2\times$  the half width at half maximum of the surface-spin linewidth ( $\approx 5$  MHz) and is much greater than the NV coupling strength to an individual spin at the surface ( $\lesssim 10$  kHz, estimated by the dipole-dipole coupling strength for two  $g = 2$  electron spins [43]). The coherence extension we observe is robust: by driving we observe a SQ  $T_2$  increase of  $>15\%$  for 11 out of 13 measured centers, and we observe up to a 140% increase.

Before further discussing the results from Fig. 2, we briefly show that the observed  $T_2$  increase is due to resonant driving of  $g = 2$  electron spins and that these spins reside at the diamond surface. Figure 3(b) plots measurements of NV coherence at fixed echo time  $2\tau$  while

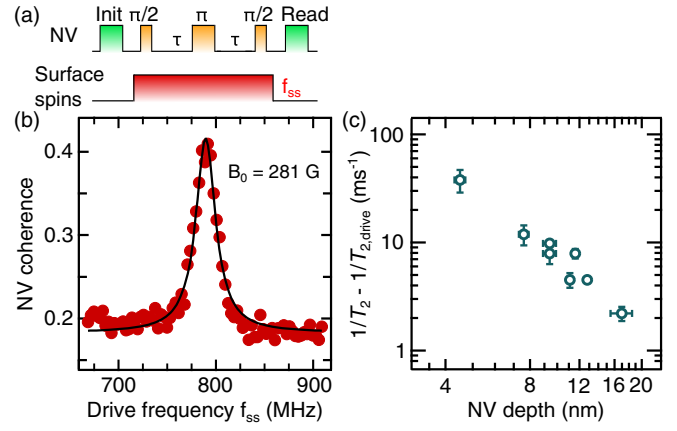


FIG. 3. NV coherence extension is due to resonant driving of  $g = 2$  electron spins at the diamond surface. (a) NV Hahn echo sequence with continuous surface-spin drive, used in (b). (b) NV Hahn echo coherence in the SQ basis at fixed  $\tau$  and varying  $f_{ss}$ , showing a resonance corresponding to  $g = 2$  spins. Black curve is a Lorentzian fit. Surface spin  $\Omega_{\text{Rabi}}/2\pi = 7$  MHz,  $2\tau = 34 \mu\text{s}$ , and the NV depth is 11.6(3) nm. (c) Decoupled SQ decoherence rate by driving at  $g = 2$  resonance, plotted as a function of NV depth. The decoupled rate is strongly anticorrelated with NV depth.

continuously driving at variable frequency  $f_{ss}$  [Fig. 3(a)]. Sweeping  $f_{ss}$  across the expected  $g = 2$  resonance (788 MHz at the applied  $B_0 = 281$  G), we observe a clear increase in the NV coherence, indicating that the coherence extension from continuous drive is due to resonant driving of  $g = 2$  spins. To confirm these spins are at the surface, in Fig. 3(c) we plot the decoupled SQ decoherence rate  $\Gamma_{\text{decoupled}} = 1/T_2 - 1/T_{2,drive}$  as a function of NV depth, measured separately on eight individual centers with depths ranging from 4 to 17 nm. We observe a strong anticorrelation between  $\Gamma_{\text{decoupled}}$  and the NV depth, with over an order of magnitude change in  $\Gamma_{\text{decoupled}}$  between the shallowest and deepest centers, demonstrating that the decoupled noise originates at the surface. We further note that on day-to-month timescales we observe order-unity variations in  $\Gamma_{\text{decoupled}}$  measured on the same NV, further indicating that the decoupled decoherence originates from the surface. Therefore,  $\Gamma_{\text{decoupled}}$  can be interpreted and utilized as a measurement of the surface-spin-induced decoherence rate. Fitting the data in Fig. 3(c) to  $\Gamma_{\text{decoupled}} \propto 1/\text{depth}^\alpha$  yields  $\alpha = 2.1(2)$ ; however, it is important to note that  $\Gamma_{\text{decoupled}}$  depends on the depth in a nontrivial way; i.e., NV centers with a different  $T_2$  probe different parts of the noise spectrum. Thus  $\Gamma_{\text{decoupled}}$  does not directly reflect the depth scaling of surface-spin-induced magnetic fluctuations  $B_{\text{rms}}^2$ , which should roughly scale as  $1/\text{depth}^4$  [6].

We now turn to a discussion of the coherence extension in the single- and double-quantum bases shown in Fig. 2. In the SQ and DQ bases, the NV has different susceptibilities to the various dephasing channels [54,55], which can be quantitatively understood by the NV's ground-state spin Hamiltonian

$$H_{\text{NV}} = (hD + d_{\parallel}\Pi_{\parallel})S_z^2 + h\frac{\gamma}{2\pi}\mathbf{S}\cdot\mathbf{B} - \frac{d_{\perp}\Pi_{\perp}}{2}(S_+^2 + S_-^2), \quad (1)$$

where  $h$  is Planck's constant,  $D = 2.87$  GHz is the crystal-field splitting,  $\mathbf{B}$  is the magnetic field,  $\mathbf{S}$  is the spin-1 operator,  $S_{\pm}$  are the spin raising and lowering operators, the  $z$  axis points along the NV axis,  $\gamma/2\pi = 2.8$  MHz/G is the NV gyromagnetic ratio,  $d_{\parallel}/h = 0.35$  and  $d_{\perp}/h = 17$  Hz cm/V are the components of the NV's electric dipole parallel and perpendicular to the  $z$  axis, and  $\Pi_{\parallel}$  and  $\Pi_{\perp}$  are the parallel and perpendicular components of the effective electric field, where  $\mathbf{\Pi} = (\mathbf{E} + \boldsymbol{\sigma})$  has both electric field  $\mathbf{E}$  and appropriately scaled strain  $\boldsymbol{\sigma}$  terms. With an applied  $\mathbf{B} = B_z\hat{z}$ , where  $(\gamma/2\pi)B_z \gg d_{\perp}\Pi_{\perp}/h$ , the Hamiltonian yields SQ transition frequencies [26,55] given by

$$f_{0\rightarrow\pm 1} \approx D + d_{\parallel}\Pi_{\parallel}/h \pm \left( \frac{\gamma}{2\pi}B_z + \frac{1}{2} \frac{(d_{\perp}\Pi_{\perp}/h)^2}{(\gamma/2\pi)B_z} \right) \quad (2)$$

and a DQ transition frequency given by

$$f_{-1\rightarrow+1} \approx 2 \left( \frac{\gamma}{2\pi}B_z + \frac{1}{2} \frac{(d_{\perp}\Pi_{\perp}/h)^2}{(\gamma/2\pi)B_z} \right). \quad (3)$$

The DQ basis has an effectively doubled gyromagnetic ratio, which has the positive effect of being more sensitive to magnetic signals, but is traded off with an increased sensitivity to magnetic noise. A clear advantage of the DQ basis, however, is the elimination of noise from the common-mode  $D + d_{\parallel}\Pi_{\parallel}/h$  terms. This advantage is borne out in Fig. 2(c) where we observe  $(T_{2,\text{DQ}}/T_{2,\text{SQ}})^n = 0.48(4)$  (where  $n = 1.6$  is the exponential stretch factor), which is greater than 0.25, the expected value for purely magnetic noise (see Supplemental Material Note 5.1 [45]), indicating the elimination of substantial common-mode noise [26].

Importantly, the advantage of operation in the DQ basis can be amplified by driving the surface spins to decouple a large portion of the magnetic environment, and in doing so, we achieve  $T_{2,\text{DQ}+\text{drive}} > T_{2,\text{SQ}}$  [Fig. 2(c)]. In result, we achieve greatly amplified sensitivity gains in magnetometry: the longer coherence time allows for a longer phase accumulation time from a magnetic signal, and the doubled gyromagnetic ratio results in a doubled phase accumulation rate [55]. To quantify these magnetometry improvements, we consider the sensitivity enhancements to incoherent ac signals, which is relevant in, e.g., noise detection of magnetic phases [17,56,57] or detection of the statistical polarization of precessing nuclear spins in nanoscale NMR [15,22,58]. In this case, the signal strength for the optically detected signal goes as  $C(T)\langle(\delta\phi)^2\rangle$ , where  $\langle(\delta\phi)^2\rangle \sim B_{\text{rms}}^2\gamma_{\text{eff}}^2T^2$  is the variance in accumulated phase,  $T$  is the total phase accumulation time,  $C(T)$  is the NV coherence,  $B_{\text{rms}}$  is the root mean square of the magnetic field, and  $\gamma_{\text{eff}}$

is the effective gyromagnetic ratio:  $\gamma_{\text{eff}} = \gamma$  in the SQ basis and  $\gamma_{\text{eff}} = 2\gamma$  in the DQ basis. Compared to a benchmark value of sensitivity, for a given measurement the sensitivity enhancement thus scales as (signal strength)/ $\sqrt{T} \sim C(T)\gamma_{\text{eff}}^2T^{3/2}$  [22].

Figure 2(d) plots the sensitivity enhancement for the data measured in Fig. 2(c), where the enhancement is relative to the peak sensitivity for the no-drive, SQ measurement. We observe a  $2\times$  sensitivity enhancement in the no-drive DQ measurement, a  $1.75\times$  enhancement in the SQ + drive measurement, and a  $5\times$  enhancement in the DQ + drive measurement. This  $5\times$  sensitivity enhancement corresponds to a  $25\times$  measurement speed-up. We note that the SQ, no-drive  $T_2$  measured here is similar to that reported for NVs of this depth [12.8(3) nm] produced by state-of-the-art materials techniques [6,44,59]; and with the enhanced collection from our diamond nanopillars, we estimate an ac magnetic field sensitivity of  $\eta_{\text{ac}} = 10$  nT Hz $^{-1/2}$  for the DQ + drive Hahn echo [24].

We now highlight a path pushing toward  $T_1$ -limited coherence times for near-surface NVs. With the advances in this work, the suspected remaining limits to shallow NV coherence in our diamond sample are  $\Pi_{\perp}$  fluctuations and bulk electron spins that produce  $B$  fluctuations. These dephasing sources can be mitigated by existing techniques that are directly complementary to the methods used in this work. First, the  $\frac{1}{2}\{[(d_{\perp}\Pi_{\perp}/h)^2]/[(\gamma/2\pi)B_z]\}$  term is suppressed with large magnetic fields. By comparing DQ and SQ coherence times at 281 G [Fig. 2(c)], we estimate the magnitude of  $\Pi_{\parallel}$  fluctuations and thereby estimate that  $\Pi_{\perp}$  fluctuations induce a  $\sim 1$  kHz dephasing rate for the NV in Fig. 2(c). We emphasize, however, that the term's nonlinearity means dephasing would be amplified beyond this estimate by static or quasistatic strain or electric fields. Second, substitutional nitrogen defects (P1 centers,  $\approx 0.3$  ppm in our implantation layer) induce magnetic fluctuations that we estimate limit DQ coherence to  $\sim 100$   $\mu\text{s}$  [60]. Lowering the implantation dosage or coherently driving the P1 centers [55,61,62] would mitigate their decohering effect. Third, nitrogen implantation induces paramagnetic vacancy clusters, which we estimate also limit DQ coherence to  $\sim 100$   $\mu\text{s}$  [59]. These defects can be prevented by gentler incorporation of nitrogen such as during diamond growth [63], or they can be removed by lattice charging during annealing [59] or high-temperature annealing [44,53,64]. We remark that any remaining dephasing would be due to magnetic sources at the diamond surface that are distinct from the coherently controlled  $g = 2$  spins in this work.

In conclusion, we demonstrate that the coherence time of a near-surface qubit is increased by coherently driving the surface electronic spins, without any additional materials processing or manipulation of the qubit. Using shallow NV centers as a model platform, we achieve a fivefold sensitivity enhancement by combining surface-spin driving

with operation in the double-quantum basis. Future work can combine the methods presented here with existing materials processing techniques to eliminate other known sources of dephasing and push toward  $T_1$ -limited coherence times for shallow NV centers. The surface-spin driving technique demonstrated here could also realize coherence extensions in other systems such as superconducting qubits, adatom qubits, and other near-surface qubits affected by surface spins. Further, these results also suggest other forms of driving as a promising path forward for near-surface qubits; for example, electrical driving of surface electric dipoles could suppress electric field noise that afflicts atoms and ions near surfaces [32,33,65].

We thank Tim Eichhorn, Nathalie de Leon, Hengyuan Zhou, Isaac Chuang, and Viatcheslav Dobrovitski for helpful discussions. We acknowledge partial support from NSF CAREER Grant No. DMR-1352660 and partial support from the DARPA DRINQS program (Agreement No. D18AC00014). D. B. acknowledges funding from the Microscopy Society of America and the Barry Goldwater Foundation.

- 
- [1] C. Wang, C. Axline, Y. Y. Gao, T. Brecht, Y. Chu, L. Frunzio, M. H. Devoret, and R. J. Schoelkopf, *Appl. Phys. Lett.* **107**, 162601 (2015).
- [2] G. S. MacCabe, H. Ren, J. Luo, J. D. Cohen, H. Zhou, A. Sipahigil, M. Mirhosseini, and O. Painter, [arXiv:1901.04129](https://arxiv.org/abs/1901.04129).
- [3] S. Baumann, W. Paul, T. Choi, C. P. Lutz, A. Ardavan, and A. J. Heinrich, *Science* **350**, 417 (2015).
- [4] Y.-J. Lin, I. Teper, C. Chin, and V. Vuletić, *Phys. Rev. Lett.* **92**, 050404 (2004).
- [5] Q. A. Turchette, D. Kielpinski, B. E. King, D. Leibfried, D. M. Meekhof, C. J. Myatt, M. A. Rowe, C. A. Sackett, C. S. Wood, W. M. Itano, C. Monroe, and D. J. Wineland, *Phys. Rev. A* **61**, 063418 (2000).
- [6] B. A. Myers, A. Das, M. C. Dartiaillh, K. Ohno, D. D. Awschalom, and A. C. Bleszynski Jayich, *Phys. Rev. Lett.* **113**, 027602 (2014).
- [7] T. Schenkel, J. A. Liddle, A. Persaud, A. M. Tyryshkin, S. A. Lyon, R. de Sousa, K. B. Whaley, J. Bokor, J. Shangkuan, and I. Chakarov, *Appl. Phys. Lett.* **88**, 112101 (2006).
- [8] S. Sendelbach, D. Hover, A. Kittel, M. Mück, J. M. Martinis, and R. McDermott, *Phys. Rev. Lett.* **100**, 227006 (2008).
- [9] H. Bluhm, J. A. Bert, N. C. Koshnick, M. E. Huber, and K. A. Moler, *Phys. Rev. Lett.* **103**, 026805 (2009).
- [10] B. K. Ofori-Okai, S. Pezzagna, K. Chang, M. Loretz, R. Schirhagl, Y. Tao, B. A. Moores, K. Groot-Berning, J. Meijer, and C. L. Degen, *Phys. Rev. B* **86**, 081406(R) (2012).
- [11] T. Rosskopf, A. Dussaux, K. Ohashi, M. Loretz, R. Schirhagl, H. Watanabe, S. Shikata, K. M. Itoh, and C. L. Degen, *Phys. Rev. Lett.* **112**, 147602 (2014).
- [12] Y. Romach, C. Müller, T. Unden, L. J. Rogers, T. Isoda, K. M. Itoh, M. Markham, A. Stacey, J. Meijer, S. Pezzagna, B. Naydenov, L. P. McGuinness, N. Bar-Gill, and F. Jelezko, *Phys. Rev. Lett.* **114**, 017601 (2015).
- [13] S. E. de Graaf, A. A. Adamyan, T. Lindström, D. Erts, S. E. Kubatkin, A. Y. Tzalenchuk, and A. V. Danilov, *Phys. Rev. Lett.* **118**, 057703 (2017).
- [14] M. W. Doherty, N. B. Manson, P. Delaney, F. Jelezko, J. Wrachtrup, and L. C. Hollenberg, *Phys. Rep.* **528**, 1 (2013).
- [15] T. Staudacher, F. Shi, S. Pezzagna, J. Meijer, J. Du, C. A. Meriles, F. Reinhard, and J. Wrachtrup, *Science* **339**, 561 (2013).
- [16] I. Gross, W. Akhtar, V. Garcia, L. J. Martínez, S. Chouaieb, K. Garcia, C. Carrétéro, A. Barthélémy, P. Appel, P. Maletinsky, J.-V. Kim, J. Y. Chauleau, N. Jaouen, M. Viret, M. Bibes, S. Fusil, and V. Jacques, *Nature (London)* **549**, 252 (2017).
- [17] F. Casola, T. van der Sar, and A. Yacoby, *Nat. Rev. Mater.* **3**, 17088 (2018).
- [18] A. Ariyaratne, D. Bluvstein, B. A. Myers, and A. C. B. Jayich, *Nat. Commun.* **9**, 2406 (2018).
- [19] A. Faraon, P. E. Barclay, C. Santori, K.-M. C. Fu, and R. G. Beausoleil, *Nat. Photonics* **5**, 301 (2011).
- [20] J. Cai, A. Retzker, F. Jelezko, and M. B. Plenio, *Nat. Phys.* **9**, 168 (2013).
- [21] D. A. Golter, T. Oo, M. Amezcua, K. A. Stewart, and H. Wang, *Phys. Rev. Lett.* **116**, 143602 (2016).
- [22] I. Lovchinsky, A. O. Sushkov, E. Urbach, N. P. de Leon, S. Choi, K. De Greve, R. Evans, R. Gertner, E. Bersin, C. Müller, L. McGuinness, F. Jelezko, R. L. Walsworth, H. Park, and M. D. Lukin, *Science* **351**, 836 (2016).
- [23] C. L. Degen, F. Reinhard, and P. Cappellaro, *Rev. Mod. Phys.* **89**, 035002 (2017).
- [24] J. M. Taylor, P. Cappellaro, L. Childress, L. Jiang, D. Budker, P. R. Hemmer, A. Yacoby, R. Walsworth, and M. D. Lukin, *Nat. Phys.* **4**, 810 (2008).
- [25] M. Pelliccione, A. Jenkins, P. Ovartchaiyapong, C. Reetz, E. Emmanouilidou, N. Ni, and A. C. Bleszynski Jayich, *Nat. Nanotechnol.* **11**, 700 (2016).
- [26] M. Kim, H. J. Mamin, M. H. Sherwood, K. Ohno, D. D. Awschalom, and D. Rugar, *Phys. Rev. Lett.* **115**, 087602 (2015).
- [27] B. A. Myers, A. Ariyaratne, and A. C. Bleszynski Jayich, *Phys. Rev. Lett.* **118**, 197201 (2017).
- [28] J. Tisler, G. Balasubramanian, B. Naydenov, R. Kolesov, B. Grotz, R. Reuter, J.-P. Boudou, P. A. Curmi, M. Sennour, A. Thorel, M. Börsch, K. Aulenbacher, R. Erdmann, P. R. Hemmer, F. Jelezko, and J. Wrachtrup, *ACS Nano* **3**, 1959 (2009).
- [29] D. Hite, Y. Colombe, A. Wilson, D. Allcock, D. Leibfried, D. Wineland, and D. Pappas, *MRS Bull.* **38**, 826 (2013).
- [30] C. M. Quintana, A. Megrant, Z. Chen, A. Dunsworth, B. Chiaro, R. Barends, B. Campbell, Y. Chen, I.-C. Hoi, E. Jeffrey, J. Kelly, J. Y. Mutus, P. J. J. O'Malley, C. Neill, P. Roushan, D. Sank, A. Vainsencher, J. Wenner, T. C. White, A. N. Cleland, and J. M. Martinis, *Appl. Phys. Lett.* **105**, 062601 (2014).
- [31] P. Kumar, S. Sendelbach, M. A. Beck, J. W. Freeland, Z. Wang, H. Wang, C. C. Yu, R. Q. Wu, D. P. Pappas, and R. McDermott, *Phys. Rev. Applied* **6**, 041001 (2016).
- [32] J. M. McGuirk, D. M. Harber, J. M. Obrecht, and E. A. Cornell, *Phys. Rev. A* **69**, 062905 (2004).

- [33] N. Daniilidis, S. Narayanan, S. A. Möller, R. Clark, T. E. Lee, P. J. Leek, A. Wallraff, S. Schulz, F. Schmidt-Kaler, and H. Häffner, *New J. Phys.* **13**, 013032 (2011).
- [34] D. A. Hite, Y. Colombe, A. C. Wilson, K. R. Brown, U. Warring, R. Jördens, J. D. Jost, K. S. McKay, D. P. Pappas, D. Leibfried, and D. J. Wineland, *Phys. Rev. Lett.* **109**, 103001 (2012).
- [35] D. Bluvstein, Z. Zhang, and A. C. Bleszynski Jayich, *Phys. Rev. Lett.* **122**, 076101 (2019).
- [36] J. Du, X. Rong, N. Zhao, Y. Wang, J. Yang, and R. B. Liu, *Nature (London)* **461**, 1265 (2009).
- [37] G. de Lange, Z. H. Wang, D. Ristè, V. V. Dobrovitski, and R. Hanson, *Science* **330**, 60 (2010).
- [38] J. Bylander, S. Gustavsson, F. Yan, F. Yoshihara, K. Harrabi, G. Fitch, D. G. Cory, Y. Nakamura, J.-S. Tsai, and W. D. Oliver, *Nat. Phys.* **7**, 565 (2011).
- [39] J. Koch, T. M. Yu, J. Gambetta, A. A. Houck, D. I. Schuster, J. Majer, A. Blais, M. H. Devoret, S. M. Girvin, and R. J. Schoelkopf, *Phys. Rev. A* **76**, 042319 (2007).
- [40] G. Wolfowicz, A. M. Tyryshkin, R. E. George, H. Riemann, N. V. Abrosimov, P. Becker, H.-J. Pohl, M. L. W. Thewalt, S. A. Lyon, and J. J. L. Morton, *Nat. Nanotechnol.* **8**, 561 (2013).
- [41] J. M. Zadrozny, A. T. Gallagher, T. D. Harris, and D. E. Freedman, *J. Am. Chem. Soc.* **139**, 7089 (2017).
- [42] A. Barfuss, J. Kölbl, L. Thiel, J. Teissier, M. Kasperczyk, and P. Maletinsky, *Nat. Phys.* **14**, 1087 (2018).
- [43] C. P. Slichter, *Principles of Magnetic Resonance* (Springer-Verlag, Berlin Heidelberg, 1990).
- [44] S. Sangtawesin, B. L. Dwyer, S. Srinivasan, J. J. Allred, L. V. H. Rodgers, K. De Greve, A. Stacey, N. Donschuk, K. M. O'Donnell, D. Hu, D. A. Evans, C. Jaye, D. A. Fischer, M. L. Markham, D. J. Twitchen, H. Park, M. D. Lukin, and N. P. de Leon, *Phys. Rev. X* **9**, 031052 (2019).
- [45] See Supplemental Material at <http://link.aps.org/supplemental/10.1103/PhysRevLett.123.146804> for supporting details on sample information, surface-spin density, rf control, the ac Stark effect, and DQ and SQ susceptibilities, which includes Refs. [46–48].
- [46] D. M. Toyli, C. D. Weis, G. D. Fuchs, T. Schenkel, and D. D. Awschalom, *Nano Lett.* **10**, 3168 (2010).
- [47] M. de Wit, G. Welker, J. M. de Voogd, and T. H. Oosterkamp, *Phys. Rev. Applied* **10**, 064045 (2018).
- [48] H. Friedrich, *Theoretical Atomic Physics*, Graduate Texts in Physics (Springer International Publishing, Cham, Switzerland, 2017), pp. 232–235.
- [49] L. M. Pham, S. J. DeVience, F. Casola, I. Lovchinsky, A. O. Sushkov, E. Bersin, J. Lee, E. Urbach, P. Cappellaro, H. Park, A. Yacoby, M. Lukin, and R. L. Walsworth, *Phys. Rev. B* **93**, 045425 (2016).
- [50] H. J. Mamin, M. H. Sherwood, and D. Rugar, *Phys. Rev. B* **86**, 195422 (2012).
- [51] M. S. Grinolds, M. Warner, K. De Greve, Y. Dovzhenko, L. Thiel, R. L. Walsworth, S. Hong, P. Maletinsky, and A. Yacoby, *Nat. Nanotechnol.* **9**, 279 (2014).
- [52] A. O. Sushkov, I. Lovchinsky, N. Chisholm, R. L. Walsworth, H. Park, and M. D. Lukin, *Phys. Rev. Lett.* **113**, 197601 (2014).
- [53] J.-P. Tetienne, R. W. de Gille, D. A. Broadway, T. Teraji, S. E. Lillie, J. M. McCoe, N. Donschuk, L. T. Hall, A. Stacey, D. A. Simpson, and L. C. L. Hollenberg, *Phys. Rev. B* **97**, 085402 (2018).
- [54] H. J. Mamin, M. H. Sherwood, M. Kim, C. T. Rettner, K. Ohno, D. D. Awschalom, and D. Rugar, *Phys. Rev. Lett.* **113**, 030803 (2014).
- [55] E. Bauch, C. A. Hart, J. M. Schloss, M. J. Turner, J. F. Barry, P. Kehayias, S. Singh, and R. L. Walsworth, *Phys. Rev. X* **8**, 031025 (2018).
- [56] L. T. Hall, J. H. Cole, C. D. Hill, and L. C. L. Hollenberg, *Phys. Rev. Lett.* **103**, 220802 (2009).
- [57] E. Schäfer-Nolte, L. Schlipf, M. Ternes, F. Reinhard, K. Kern, and J. Wrachtrup, *Phys. Rev. Lett.* **113**, 217204 (2014).
- [58] C. A. Meriles, L. Jiang, G. Goldstein, J. S. Hodges, J. Maze, M. D. Lukin, and P. Cappellaro, *J. Chem. Phys.* **133**, 124105 (2010).
- [59] F. Fávoro de Oliveira, D. Antonov, Y. Wang, P. Neumann, S. A. Momenzadeh, T. Häußermann, A. Pasquarelli, A. Denisenko, and J. Wrachtrup, *Nat. Commun.* **8**, 15409 (2017).
- [60] E. Bauch, S. Singh, J. Lee, C. A. Hart, J. M. Schloss, M. J. Turner, J. F. Barry, L. Pham, N. Bar-Gill, S. F. Yelin, and R. L. Walsworth, [arXiv:1904.08763](https://arxiv.org/abs/1904.08763).
- [61] G. de Lange, T. van der Sar, M. Blok, Z.-H. Wang, V. Dobrovitski, and R. Hanson, *Sci. Rep.* **2**, 382 (2012).
- [62] H. S. Knowles, D. M. Kara, and M. Atatüre, *Nat. Mater.* **13**, 21 (2014).
- [63] K. Ohno, F. Joseph Heremans, L. C. Bassett, B. A. Myers, D. M. Toyli, A. C. Bleszynski Jayich, C. J. Palmstrøm, and D. D. Awschalom, *Appl. Phys. Lett.* **101**, 082413 (2012).
- [64] T. Yamamoto, T. Umeda, K. Watanabe, S. Onoda, M. L. Markham, D. J. Twitchen, B. Naydenov, L. P. McGuinness, T. Teraji, S. Koizumi, F. Dolde, H. Fedder, J. Honert, J. Wrachtrup, T. Ohshima, F. Jelezko, and J. Isoya, *Phys. Rev. B* **88**, 075206 (2013).
- [65] J. A. Sedlacek, J. Stuart, D. H. Slichter, C. D. Bruzewicz, R. McConnell, J. M. Sage, and J. Chiaverini, *Phys. Rev. A* **98**, 063430 (2018).